A tabular optimisation technique for steel lazy wave riser

A. M. Ogbeifun[1], S. Oterkus[1], J. Race[1], H. Naik[2], D. Moorthy[3], S. Bhowmik[2], J. Ingram[3]

[1]Naval Architecture, Ocean and Marine Engineering, University of Strathclyde, Glasgow, G4 0LZ, UK.
[2]McDermott International, 40 Eastbourne Terrace, Paddington, London, W2 6LG, UK.
[3]McDermott International, 757 N. Eldridge Parkway, Houston, TX 77079, USA.

Abstract. Steel lazy wave riser (SLWR) is derived from the simple catenary riser (SCR) by the installation of buoyancy modules on its section. Infinite SLWR configurations are possible, and this poses difficulties in determining the best configuration. However, it is possible to capture some suitable configurations which satisfy some given design criteria specific to a project. We referred to these as the optimum configurations for the problem. Several advanced optimization tools and techniques for engineering optimization are available. In this paper, we present a 2D tabular optimization method for SLWR, which is an index-based optimization technique. The approach reduces a multidimensional problem to a 2D type providing a significant reduction in the required computational resources. It combines the design variables in pairs and assigns indices to the resulting design points (configurations) for each combination. The optimum design points are then tracked through index matching using techniques such as data sorting and intersection operations. In the application of the technique to SLWR design, we set the number of design variable for the problem to three. This results in three pair of combinations of the design variables. The design variables are the apparent mass ratio, the sag bend elevation, and the arc height. The output variables of interest to be optimized include the SLWR hanging length, the smeared buoyancy section length, the smeared buoyancy thickness, the riser hang-off tension, the stress utilization and fatigue damage around the bends. Selected optimum SLWR configurations from the optimization process are subjected to an irregular wave simulation to demonstrate the suitability of the approach for such optimisation problems.

1. Introduction

Riser systems are required to transport production fluid between the seabed and the floating production vessel. Risers are the most challenging components in deep-water oil and gas developments because of their extreme dynamic response. The steel catenary riser (SCR) is one of the riser type, which assumes a free hanging catenary configuration between its connecting point to the floating production vessel and the touchdown point (TDP), where it first contacts the seabed. SCRs are attractive riser systems [1] and have been used in many field developments considering their simplicity and relatively lower delivery cost compared to other riser system types [2-4]. However, when subjected to dynamic conditions, the SCR is limited by the high stress and fatigue damage responses experienced around critical sections, which are the hang off (HO) region and the touchdown zone (TDZ) [5], shown in Figure 1. The efforts made to reduce the stress and fatigue responses include but not limited to changing the configuration of SCR by including buoyancy modules on its sections,

applying alternative material with better properties compared with steel and developing better riser interaction models to reduce design conservativism [6].

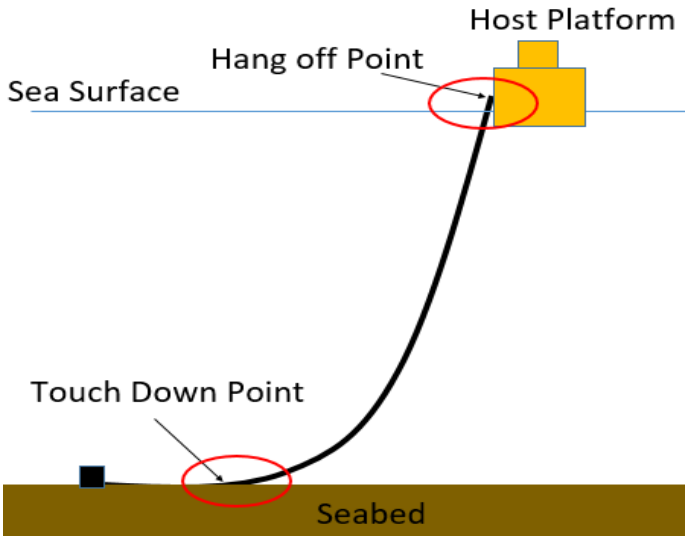

Figure 1. Conventional steel catenary riser schematic [6].

The SLWR solution is derived from SCR configuration by installing buoyancy modules on sections of the riser. The installed buoyancy modules induce compliant bends or 'waves' which help to decouple the vessel motion from the riser TDZ, resulting in the reduction of the stress and fatigue responses. The upward pull of the buoyancy modules on the SLWR section also helps to reduce the riser submerged weight and top tension. The level of benefits that can be derived from SLWR (over SCR) depends on an appropriate combination of its configuration variables. These include the buoyancy module capacity and lengths, the arc height, and the sag bend elevation of the SLWR. Several combinations of the configuration variables are possible, resulting in infinite possible SLWR configurations. However, suitable configurations satisfying a given project design criteria are usually searched for.

This paper presents a simplified 2D tabular optimization approach used to capture a family of suitable SLWR configurations, from the problem's design optimization space. The design space characterized by multi-dimension (3D) is reduced to three 2D spaces defined by a combination of pairs of the three independent configuration variables. These variables are the apparent mass ratio (AMR), the sag elevation (y_{sag}) and the arc height (Δh). Note that for the SLWR example in this paper, a fixed water depth and riser hang-off angle is considered. Unique indices are then assigned to the design points (SLWR configurations) in each of the three 2D design spaces. Output variables (response and geometric variables) are post-processed, arranged in tables, and sorted either in ascending or descending order for minimisation or maximization problems, respectively. The index tables corresponding to the output variables tables are re-arranged accordingly to match the repositioned output variable values in the sorted result tables. The first user-defined number of intersections of the re-arranged index tables point to the family of optimum SLWRs configurations. The detailed procedure for this technique is presented in the methodology section. An example of the SLWR optimization problem is presented in this paper to demonstrate the development, application, and suitability of the tabular optimization technique, which is considered to simplify a supposed complex optimisation process.

2. Methodology

2.1. Lazy wave configuration calculation

A typical SLWR configuration is presented in Figure 2. The highest and the lowest points on the 'wave' bend are referred to as the 'hog' and the 'sag' bend elevations from the seabed, denoted as y_{hog} and y_{sag} respectively. They are related by equation (1), where Δh is the arch height of the SLWR.

$$y_{hog} = y_{sag} + \Delta h \tag{1}$$

Different combinations of y_{sag}, Δh, the height of SLWR (h), the riser hang-off angle with the horizontal (θ) and the buoyancy section capacity results in different SLWR configurations. An example of possible input combinations options for specifying SLWR configurations is given in Table 1 [7]. It should be noted that for a unique SLWR configuration, any of the two input options in Table 1 can be re-expressed in the form of the other through the catenary equations. Option-1 is used in this paper.

Table 1. Design input options for LWR configuration.

Options	Δh	y_{sag}	Section lengths	θ	h
1	✔	✔	-	✔	✔
2	-	-	✔	✔	✔

The SLWR system configuration shown in Figure 2 (a), can be decomposed into five (5) sub catenaries, each with their local coordinate, as shown in Figure 2 (b). The catenary equations used for calculating each sub catenary are presented in equations (2) to (7). The horizontal top tension component (H) is constant everywhere along the SLWR profile, and this ensures continuity in the profile curvature. These equations are used to define the initial configuration of the SLWR for the finite element modelling. The equations are developed based on the assumption that the line has infinite axial stiffness and negligible bending stiffness.

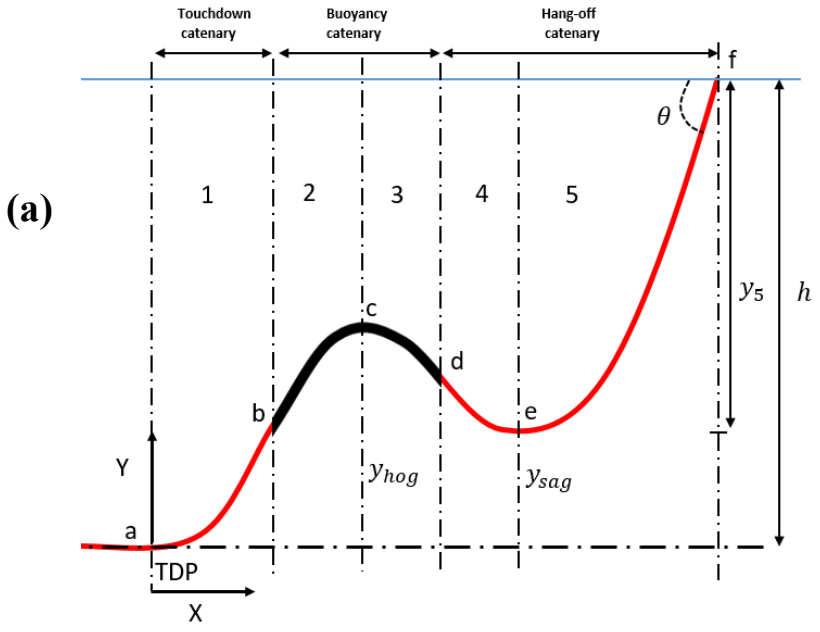

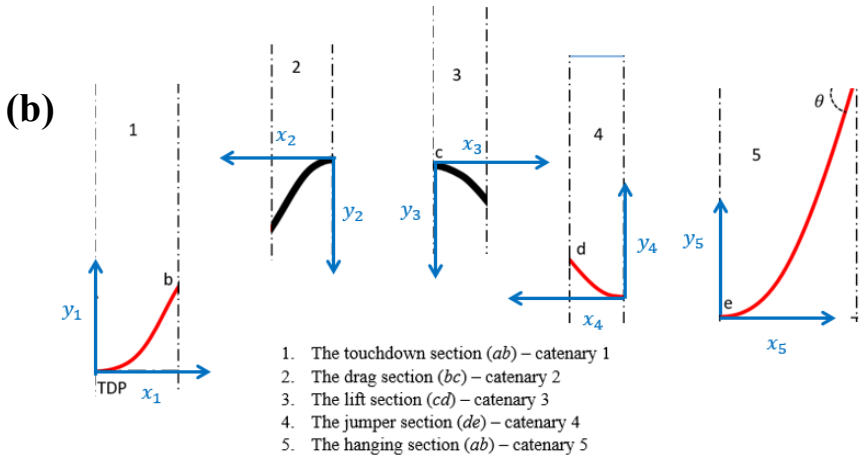

Figure 2. Steel lazy wave riser (SLWR) configuration: (a) Global configuration of SLWR, (b) Sub catenaries of the SLWR global configuration

$$\begin{cases} H = H_5 = \dfrac{wy_5}{(\tan\theta)^2}(1+\sec\theta) \\ x_5 = \dfrac{H}{w}\cosh^{-1}\left(\dfrac{wy_5}{H}+1\right) \\ s_5 = \dfrac{H}{w}\sinh\left(\dfrac{wx_5}{H}\right) \end{cases} \tag{2}$$

$$\begin{cases} y_4 = \dfrac{w_b}{w+w_b}(y_{hog}-y_{sag}) \\ x_4 = \dfrac{H}{w}\cosh^{-1}\left(\dfrac{wy_4}{H}+1\right) \\ s_4 = \dfrac{H}{w}\sinh\left(\dfrac{wx_4}{H}\right) \end{cases} \tag{3}$$

$$\begin{cases} y_3 = \dfrac{w}{w+w_b}(y_{hog}-y_{sag}) \\ x_3 = \dfrac{H}{w}\cosh^{-1}\left(\dfrac{w_by_3}{H}+1\right) \\ s_3 = \dfrac{H}{w_b}\sinh\left(\dfrac{w_bx_3}{H}\right) \end{cases} \tag{4}$$

$$\begin{cases} y_2 = \dfrac{w}{w+w_b}y_{hog} \\ x_2 = \dfrac{H}{w_b}\cosh^{-1}\left(\dfrac{w_by_2}{H}+1\right) \\ s_2 = \dfrac{H}{w_b}\sinh\left(\dfrac{w_bx_2}{H}\right) \end{cases} \tag{5}$$

$$\begin{cases} y_1 = \dfrac{w_b}{w + w_b} y_{hog} \\ x_1 = \dfrac{H}{w} cosh^{-1}\left(\dfrac{w y_1}{H} + 1\right) \\ s_1 = \dfrac{H}{w} sinh\left(\dfrac{w x_1}{H}\right) \end{cases} \tag{6}$$

$$X_T = \sum_{i=1}^{5} x_i \,;\;\; h = \sum_{i=1}^{5} y_i \,;\; S_T = \sum_{i=1}^{5} s_i \tag{7}$$

Where s_i, x_i, y_i and H_i are respectively the catenary length, the horizontal span, the vertical span and the horizontal tension components of the i^{th} sub catenary; X_T and S_T are respectively the total horizontal span, and the total riser length from hang-off (HO) to TDP; w and w_b are respectively the submerged unit weight of the bare pipe and the buoyant sections; and θ is the HO angle with the horizontal. The buoyant section capacity is determined by the thickness (or diameter), length, material density and the number of the discrete buoyancy modules installed on the SLWR. For a given buoyancy capacity, buoyancy material density and different values of the buoyancy module thickness (or diameter), there will be different corresponding lengths of the buoyant section. In this work, the discrete buoyancy section is conveniently modelled as an equivalent smeared buoyancy section. This is achieved by deriving an equivalent smeared buoyancy diameter that will provide equal displacements as all the discrete buoyancy modules. The thickness (t_b) or diameter (D_b) of the smeared buoyant section is modelled as the apparent mass ratio (AMR) as will be seen in the next section. Where $2t_b = D_b - D_o$, D_o is the bare pipe section outer diameter.

2.2. Concept of apparent mass ratio (AMR)

The apparent mass ratio (AMR) is the ratio of the apparent or submerged weight of the buoyant section, w_b, to the apparent or submerged weight of the bare pipe section, w

$$AMR = \frac{w_b}{w} = \frac{w_p + w_c + w_m - B_b}{w_p + w_c - B_p} \tag{8}$$

Where w_p, w_c, w_m, B_b and B_p are respectively the unit weight of bare pipe, unit weight of riser content, unit weight of buoyancy material, unit buoyancy force provided by the buoyant section and unit buoyancy force provided by the bare pipe section. Equation (8) can be expanded and re-casted as equation (9), which provides a relationship between the AMR, the buoyancy material density (ρ_b) and the smeared buoyant section thickness (t_b). The positive real roots of equation (9) gives the required, t_b for a given AMR and ρ_b. Where D_i and D_o are the inner and outer diameters of the bare pipe section, ρ_c and ρ_w are respectively the content and seawater density.

$$At_b^2 + Bt_b + C = 0 \tag{9}$$

Where:

$$A = 4(\rho_b - \rho_w), B = 4D_o(\rho_b - \rho_w)$$

$$C = (1 - AMR)\,(\rho_s D_o^2 - \rho_s D_i^2 + \rho_c D_i^2 - \rho_w D_o^2)$$

The calculated t_b is used to determine w_b which is substituted into the catenary equations for the SLWR configuration calculation, for a given $y_{sag}, \Delta h,$ and θ.

2.3. 2D tabular optimisation methodology

For fixed values of the SLWR HO angle with the horizontal, θ and the height of the SLWR, h, let **X** be the vector of design input variables i.e. $X_1 = y_{sag}$, $X_2 =$ AMR, and $X_3 = \Delta h$. Let **Y** be the design output variables to be optimised i.e. $Y_1 = U_{bend}$, $Y_2 = T_{top}$, $Y_3 = \Delta\sigma_{bend}$, $Y_4 = s_b$, $Y_5 = t_b$ and $Y_6 = S_T$. The optimization problem can be expressed as follows:

$$\text{find } \mathbf{X} = \begin{Bmatrix} AMR \\ y_{sag} \\ \Delta h \end{Bmatrix} \text{ which minimizes } \mathbf{Y} = \begin{Bmatrix} U_{bend} \\ T_{top} \\ \Delta\sigma_{bend} \\ s_b \\ S_T \\ t_b \end{Bmatrix} \tag{10}$$

Subject to the following constraints:

$$AMR < 0, y_{sag} > 0, \Delta h \geq 0$$

Where AMR is the apparent mass ratio of the buoyant sections, y_{sag} is the sag height elevation from the seabed, Δh is the arc height, U_{bend} is the stress utilization in the riser bends, T_{top} is the tension the riser top, $\Delta\sigma_{bend}$ is the stress range in the riser bends (representative of the fatigue damage), s_b is the smeared buoyant section length, S_T is the total hanging length of the SLWR, and t_b is the smeared buoyant section thickness.

From the optimization problem layout, there are three independent design input variables (m =3) and six design output variables (p = 6). The 2D tabular approach presented in this paper requires the joint variation of two (2) variables, while the third is set to an arbitrary practical value. Hence, there will be three combination pairs ($n = \mathrm{C}(m, 2) = \mathrm{C}(3,2) = 3$), referred to as the design configurations groups. The number of result tables (denoted as $Y_{p,n}$) will then be $p \times n$. A system of index tables (denoted as $I_{p,n}$) is created of equal dimension with $Y_{p,n}$ to represent the index locations of all results in the tables of $Y_{p,n}$. The layout of the results tables, $Y_{p,n}$ and the index system tables, $I_{p,n}$ are presented in Table 2 and Table 3, respectively. For numerical convenience, each table in $Y_{p,n}$ and $I_{p,n}$ can be converted to columns or vectors, and from this point on can be interchangeably referred to as *result columns* and *index columns* in $Y_{p,n}$ and $I_{p,n}$ respectively.

Table 2. Result tables in each configuration groups.

Configuration group		Output variable tables or columns ($Y_{p,n}$)					
		U_{bend}	T_{top}	$\Delta\sigma_{bend}$	s_b	S_T	t_b
y_{sag}, AMR	$Y_{p,n=1}$	$Y_{1,1}$	$Y_{2,1}$	$Y_{3,1}$	$Y_{4,1}$	$Y_{5,1}$	$Y_{6,1}$
$\Delta h, AMR$	$Y_{p,n=2}$	$Y_{1,2}$	$Y_{2,2}$	$Y_{3,2}$	$Y_{4,2}$	$Y_{5,2}$	$Y_{6,2}$
$y_{sag}, \Delta h$	$Y_{p,n=3}$	$Y_{1,3}$	$Y_{2,3}$	$Y_{3,3}$	$Y_{4,3}$	$Y_{5,3}$	$Y_{6,3}$

Table 3. Index tables system.

Configuration groups		Index system tables or columns ($I_{p,n}$)					
		U_{bend}	T_{top}	$\Delta\sigma_{bend}$	s_b	S_T	t_b
y_{sag}, AMR	$I_{p,1}$	$I_{1,1}$	$I_{2,1}$	$I_{3,1}$	$I_{4,1}$	$I_{5,1}$	$I_{6,1}$
$\Delta h, AMR$	$I_{p,2}$	$I_{1,2}$	$I_{2,2}$	$I_{3,2}$	$I_{4,2}$	$I_{5,2}$	$I_{6,2}$
$y_{sag}, \Delta h$	$I_{p,3}$	$I_{1,3}$	$I_{2,3}$	$I_{3,3}$	$I_{4,3}$	$I_{5,3}$	$I_{6,3}$

Every table (or result column) in $Y_{p,n}$ are sorted in ascending order (for minimisation problem) or descending order for maximisation problems. The corresponding tables (or index columns) in $I_{p,n}$ are

likewise re-arranged accordingly to match the repositioned output variable values in the sorted tables in $Y_{p,n}$. Intersection operation is carried out on the re-arranged index columns, and the first user-specified number of index intersections, k, point to a family of optimum SLWRs configurations. The k indices of the optimum SLWR configurations can be generally expressed as equation (11) and depicted in Figure 3, where P is the total number of output variables and N is the total number of pair combinations of the input variables.

$$\bigcap\left(I_{p,n}\right)_k, 1 \le p \le P \text{ and } 1 \le n \le N \tag{11}$$

A subset of the intersection in equation (11) can also be searched for. For example, if there is need to know what configurations optimizes U_{bend} (p =1) and s_b (p =4), then equation (12) applies.

$$\bigcap\left(I_{p,n}\right), p = 1, 4 \text{ and } 1 \le n \le 3 \tag{12}$$

The k indices of optimum family members obtained can then be matched to the design and result space to determine the corresponding optimum design variables, which are the AMR, y_{sag} and Δh, and the corresponding values of the design output variable, which are U_{bend}, T_{top}, $\Delta\sigma_{bend}$, s_b, S_T and t_b.

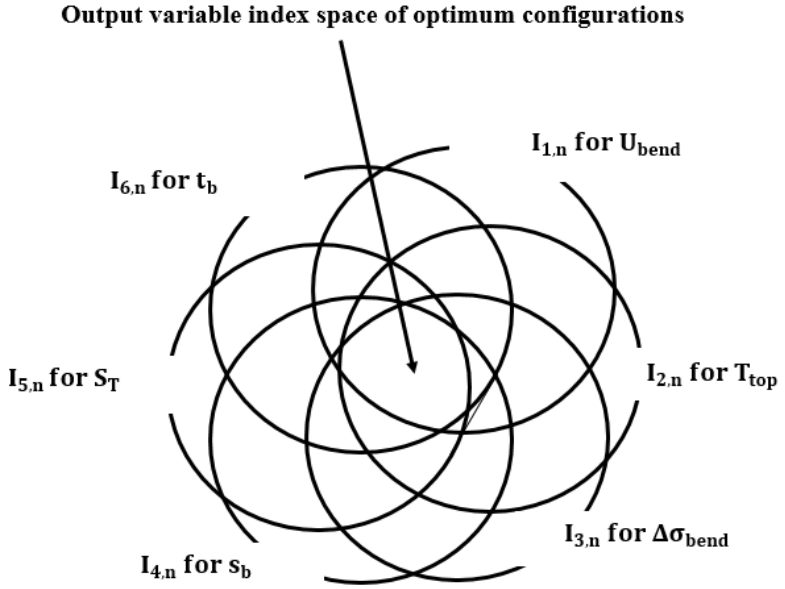

Figure 3. Optimum configuration index space intersections.

3. Analysis data

3.1. Riser model

The SLWR used for this study is made up of a string of 12-inch X70 grade pipes. It is hosted by a generic floating production, storage, and offloading (FPSO) unit at an azimuth of 90deg to the vessel heading. The minimum wall thickness required for burst and collapse pressure resistance was calculated using DNV-OS-F201 criteria [8]. Table 4 presents the design data for the riser.

Table 4. Riser data.

SLWR data	Values
Pipe size	12inch
Internal Design pressure	10ksi
Pipe thickness (fixed)	27.5mm
Hang off angle with the vertical (fixed)	$(90 - \theta) = 12^{o}$
Content density	600kg/m3
Hang off stiffness (linear)	12kN.m/deg
Buoyancy material density	500kg/m^3
Water depth	1500m
Buoyant section length	Vary (m) (based on varying AMR)
Smeared buoyancy thickness	Vary (m) (based on varying AMR)
Total riser length	Vary (m)

The design range of values for each of the design input variables consist of 14 entries (design points) presented in Table 5.

Table 5. Design input variable space.

y_{sag}(m)	AMR	Δh(m)	y_{sag}(m)	AMR	Δh(m)
10	-0.10	0	430	-1.75	280
70	-0.25	40	490	-2.00	320
130	-0.50	80	550	-2.25	360
190	-0.75	120	610	-2.50	400
250	-1.00	160	670	-2.75	440
310	-1.25	200	730	-3.00	480
370	-1.50	240	790	-3.25	520

3.2. Environmental, vessel and seabed data

Two irregular wave loads for the combined load and fatigue analysis are presented in Table 6. The optimisation stage is a screening process where hundreds of FE models are simulated to search for a family of optimum configurations. Applying irregular wave loads for the combined load and fatigue analysis during the optimisation process may be prohibitive as huge computation resources will be required to do so. Hence, the equivalent regular wave load data are used during the optimisation stage. Once a family of the optimum SLWR configurations are obtained, the selected optimum configurations will be subjected to the irregular wave analysis for a minimum of 3hrs period.

Table 6. Wave load data.

Analyses	Wave type	Data	Values
Combined	Irregular wave	H_s(m)	8
		T_p(sec)	13
		γ	1.6
	Equivalent regular wave	H_{max}(m)	14.9
		T(sec)	9.5
Fatigue	Irregular wave	H_s(m)	4.5
		T_p(sec)	9.5
		γ	1.8
	Equivalent regular wave	H_{max}(m)	8.4
		T(sec)	7

The equivalent regular wave loads are calculated from the irregular wave loads using equations (13) and (14), where T is the regular wave period, H_{max} is the probable maximum wave height, T_z is the irregular wave zero up crossing period, T_p is the wave peak period and γ is the wave peak shape parameter. Both equations are valid for the JONSWAP spectrum with wave peak shape parameter in the range $1 \leq \gamma < 7$ [9]. All wave loads are considered Beam Sea and current loads are excluded.

$$H_{max} = 1.86H_s, T = T_z \tag{13}$$

$$T_z = T_p(0.6673 + 0.05037\gamma - 0.006230\gamma^2 + 0.0003341\gamma^3) \tag{14}$$

A generic response amplitude operator (RAOs) for the FPSO is implemented. The nonlinear hysteretic riser soil interaction model is used. Details of the default riser soil interaction model data used can be found in [10].

4. Analysis, results, and discussion

4.1. Analysis method

As presented in Table 5, each of the three design variables has 14 entries. There are $n = 3$ combination pairs or configuration groups of the design variables presented in Table 7, resulting in a total number of $2 \times 14 \times 14$ =588 design points. For each of the configuration group, an arbitrary practical value for the third variable is set. As seen in Table 7, $\Delta h = 50m$ for group 1, $y_{sag} = 100m$ for group 2 and $AMR = -1$ for group 3. FE model for each of the 588 design points are built and simulated for both the combined and the fatigue regular wave loads. The numerical simulations of the models were conducted using the OrcaFlex FE software package[11]. Modelling, pre-processing, post-processing, result organisation in tables of $Y_{p,n}$ and the setting up of the corresponding index tables in $I_{p,n}$ are automated using MATLAB/PYTHON programs integrated with OrcaFlex programming interface (OrcFxAPI [12]). The program generates the OrcaFlex models using the equation (2) to equation (7) to define the SLWRs initial configurations.

Table 7. Input variable combination (Configuration groups).

Conf. Group1 $\Delta h = 50$m		Conf. Group2 $y_{sag} = 100$m		Conf. Group3 AMR = -1	
y_{sag}(m)	AMR	Δh(m)	AMR	y_{sag}(m)	Δh(m)
10	-0.10	0	-0.10	10	0
70	-0.25	40	-0.25	70	40
130	-0.50	80	-0.50	130	80
190	-0.75	120	-0.75	190	120
250	-1.00	160	-1.00	250	160
310	-1.25	200	-1.25	310	200
370	-1.50	240	-1.50	370	240
430	-1.75	280	-1.75	430	280
490	-2.00	320	-2.00	490	320
550	-2.25	360	-2.25	550	360
610	-2.50	400	-2.50	610	400
670	-2.75	440	-2.75	670	440
730	-3.00	480	-3.00	730	480
790	-3.25	520	-3.25	790	520

For each model, the output variables: the stress utilization (U_{bend}), the top tension (T_{top}), the stress range ($\Delta\sigma_{bend}$) and the SLWR geometry or dimension (t_b, S_T and s_b) are obtained. Note that stress

utilization is calculated based on DNV-OS-F201, considering the combined load resistance factor design criteria for internal and external overpressure conditions [8]. The output ($p = 6$) variables are post-processed, and their extreme or maximum values are obtained and organised in tables in $Y_{p,n}$. The number of result tables or columns in $Y_{p,n}$ will be $n \times p = 18$ (see Table 5). The corresponding system of index tables $I_{p,n}$ will also contain 18 tables or result columns. Figure 6 (a), (b) and (c) present the 2D spatial representation of Table 7, showing the design space index of the three-design variable combination or configuration groups. The design variable values are shaded in 'blue'.

AMR

$y_{sag}(m)$	-0.1	-0.25	-0.5	-0.75	-1	-1.25	-1.5	-1.75	-2	-2.25	-2.5	-2.75	-3	-3.25
10	1	15	29	43	57	71	85	99	113	127	141	155	169	183
70	2	16	30	44	58	72	86	100	114	128	142	156	170	184
130	3	17	31	45	59	73	87	101	115	129	143	157	171	185
190	4	18	32	46	60	74	88	102	116	130	144	158	172	186
250	5	19	33	47	61	75	89	103	117	131	145	159	173	187
310	6	20	34	48	62	76	90	104	118	132	146	160	174	188
370	7	21	35	49	63	77	91	105	119	133	147	161	175	189
430	8	22	36	50	64	78	92	106	120	134	148	162	176	190
490	9	23	37	51	65	79	93	107	121	135	149	163	177	191
550	10	24	38	52	66	80	94	108	122	136	150	164	178	192
610	11	25	39	53	67	81	95	109	123	137	151	165	179	193
670	12	26	40	54	68	82	96	110	124	138	152	166	180	194
730	13	27	41	55	69	83	97	111	125	139	153	167	181	195
790	14	28	42	56	70	84	98	112	126	140	154	168	182	196

Vectorized indices

Figure 4. Conf. Group 1: Joint variation of y_{sag} and AMR.

AMR

$\Delta h(m)$	-0.1	-0.25	-0.5	-0.75	-1	-1.25	-1.5	-1.75	-2	-2.25	-2.5	-2.75	-3	-3.25
0	1	15	29	43	57	71	85	99	113	127	141	155	169	183
40	2	16	30	44	58	72	86	100	114	128	142	156	170	184
80	3	17	31	45	59	73	87	101	115	129	143	157	171	185
120	4	18	32	46	60	74	88	102	116	130	144	158	172	186
160	5	19	33	47	61	75	89	103	117	131	145	159	173	187
200	6	20	34	48	62	76	90	104	118	132	146	160	174	188
240	7	21	35	49	63	77	91	105	119	133	147	161	175	189
280	8	22	36	50	64	78	92	106	120	134	148	162	176	190
320	9	23	37	51	65	79	93	107	121	135	149	163	177	191
360	10	24	38	52	66	80	94	108	122	136	150	164	178	192
400	11	25	39	53	67	81	95	109	123	137	151	165	179	193
440	12	26	40	54	68	82	96	110	124	138	152	166	180	194
480	13	27	41	55	69	83	97	111	125	139	153	167	181	195
520	14	28	42	56	70	84	98	112	126	140	154	168	182	196

Vectorized indices

Figure 5. Conf. Group 2: Joint variation of y_{sag} and Δh.

Δh(m)

$y_{sag}(m)$	0	40	80	120	160	200	240	280	320	360	400	440	480	520
10	1	15	29	43	57	71	85	99	113	127	141	155	169	183
70	2	16	30	44	58	72	86	100	114	128	142	156	170	184
130	3	17	31	45	59	73	87	101	115	129	143	157	171	185
190	4	18	32	46	60	74	88	102	116	130	144	158	172	186
250	5	19	33	47	61	75	89	103	117	131	145	159	173	187
310	6	20	34	48	62	76	90	104	118	132	146	160	174	188
370	7	21	35	49	63	77	91	105	119	133	147	161	175	189
430	8	22	36	50	64	78	92	106	120	134	148	162	176	190
490	9	23	37	51	65	79	93	107	121	135	149	163	177	191
550	10	24	38	52	66	80	94	108	122	136	150	164	178	192
610	11	25	39	53	67	81	95	109	123	137	151	165	179	193
670	12	26	40	54	68	82	96	110	124	138	152	166	180	194
730	13	27	41	55	69	83	97	111	125	139	153	167	181	195
790	14	28	42	56	70	84	98	112	126	140	154	168	182	196

Vectorized indices

Figure 6. Conf. Group 3: Joint variation of AMR and Δh.

4.2. Results and discussion

Recall from Table 2 that each of the ($n = 3$) configuration group contains six result tables or columns, corresponding to each of the ($p = 6$) design output variables. This gives 18 result columns in $Y_{p,n}$. Similarly, there will be 18 associated index tables or columns in $I_{p,n}$ as seen in Table 3. First, the 18 index tables or columns in $I_{p,n}$ are sorted in ascending order, and the associated index tables in $I_{p,n}$ are rearranged accordingly. The intersection of the index columns for each configuration group is then obtained. The second, third and fourth columns of Table 8 present the intersections of tables or index columns in each of the three configuration group. They are respectively $\cap(I_{p,1}), \cap(I_{p,2})$ and $\cap(I_{p,3})$. The configuration indices in these columns are pointers to optimum SLWR configurations for the groups. The fifth column presents the combined intersection of the three configuration groups, i.e.:

$$\cap(I_{p,n}) = \cap(I_{p,1}, I_{p,2}, I_{p,3}), \qquad 1 \le p \le 6 \tag{15}$$

Table 8. Index numbers intersection (pointers) to optimum configurations.

	Conf. group 1	Conf. group 2	Conf. group 3	Combined
92	[]	[]	[]	[]
93	[]	[]	[]	[]
94	[]	[]	78	[]
95	[]	[]	78	[]
96	[]	[]	[78;92]	[]
97	[]	[]	[78;92]	[]
98	[]	[]	[78;92]	[]
99	[]	[]	[78;91;92]	[]
100	[]	[]	[77;78;91;92]	[]
101	[]	[]	[77;78;91;92]	[]
102	[]	[]	[77;78;91;92]	[]
103	[]	[]	[63;77;78;91;92]	[]
104	[]	[]	[63;77;78;91;92]	[]
105	[]	[]	[63;64;77;78;91;92]	[]
106	[]	86	[63;64;77;78;91;92]	[]
107	[]	[73;86;107]	[63;64;77;78;91;92]	[]
108	[]	[73;86;107]	[63;64;77;78;91;92]	[]
109	[]	[73;86;101;107]	[63;64;77;78;91;92]	[]
110	[]	[73;86;87;101;107]	[63;64;77;78;91;92;106]	[]
111	[]	[73;86;87;101;107]	[63;64;77;78;79;91;92;106]	[]
112	[]	[73;86;87;101;107]	[63;64;77;78;79;91;92;93;106]	[]
113	91	[73;86;87;101;107]	[63;64;77;78;79;91;92;93;105;106]	[]
114	91	[73;86;87;101;107;108]	[63;64;77;78;79;90;91;92;93;105;106]	[]
115	91	[73;86;87;92;101;107;108]	[48;63;64;77;78;79;90;91;92;93;105;106;107]	[]
116	[91;107]	[73;86;87;92;101;107;108]	[48;63;64;77;78;79;90;91;92;93;105;106;107]	107
117	[91;107]	[73;86;87;92;101;107;108]	[48;63;64;77;78;79;90;91;92;93;105;106;107]	107
118	[91;107]	[73;86;87;92;101;107;108]	[48;62;63;64;77;78;79;90;91;92;93;105;106;107]	107
119	[91;94;107]	[73;86;87;92;93;101;107;108]	[48;62;63;64;77;78;79;90;91;92;93;104;105;106;107]	107
120	[91;94;107]	[73;86;87;92;93;101;107;108]	[48;62;63;64;76;77;78;79;90;91;92;93;104;105;106;107]	107
121	[91;94;107]	[73;86;87;92;93;101;107;108;121]	[48;62;63;64;76;77;78;79;90;91;92;93;104;105;106;107]	107
122	[91;94;95;107;108]	[73;86;87;92;93;101;107;108;115;121;122]	[48;62;63;64;76;77;78;79;90;91;92;93;104;105;106;107]	107
123	[91;92;94;95;107;108]	[73;86;87;92;93;101;107;108;115;121;122]	48;62;63;64;76;77;78;79;90;91;92;93;104;105;106;107;108	[92;107;108]
124	[91;92;94;95;107;108]	3;86;87;92;93;101;107;108;115;121;122;12	62;63;64;76;77;78;79;90;91;92;93;104;105;106;107;108;1	[92;107;108]

.

From Table 8, the following points should be noted:

- Configuration index 91 appears as the first configuration, which optimises all six output variables in configuration group 1. In Figure 4, Index 91 matches SLWR configuration with AMR = -1.5 and y_{sag} =370m. Index 91 occurs in the first k = 113 row search across the six index columns of configuration group 1 ($Y_{p,1}$). As k increases beyond 115, more configurations index such as 107, 94, 95, 108, etc. is included in the family of optimum SLWR in configuration group 1.
- Configuration index 86 appears as the first configuration, which optimises all six output variables in configuration group 2. In Figure 5, Index 86 matches SLWR configuration with AMR = -1.5 and Δh =40m. Index 86 occurs in the first k = 106 row search across the six index columns of configuration group 2 ($Y_{p,2}$). As k increases beyond 106, more configurations index such as 73, 107, 87,101, etc. is included in the family of optimum SLWR in configuration group 2.

- Configuration index 78 appears as the first configuration, which optimises all six output variables in configuration group 3. In Figure 6, Index 78 matches SLWR configuration with Δh = 200 and y_{sag} =430m. Index 78 occurs in the first k = 94 row search across the six index columns of configuration group 3 ($Y_{p,3}$). As k increases beyond 95, more configurations index such as 92, 91, 77, 63, etc. is included in the family of optimum SLWR in configuration group 3.
- Configuration index 107 appears as the first configuration, which optimises all six output variables in all three configuration groups (Group 1, 2 and 3). Index 107 occurs in the first k = 116 row search across the six index columns vectors of all three configuration groups as indicated by equation (15). Since index 107 is a result of the intersection of the index columns across the three groups, we must therefore match it against the three configuration group design spaces presented respectively in Figure 4, Figure 5 and Figure 6. By doing so, we find out that index 107 matches with the SLWR configurations with y_{sag} = 490m, AMR = -1.75, Δh =320m, 280m. Note that two Δh values occur since Δh appears as the row header in Figure 5 and the column header Figure 6. As k increases beyond 122, more configurations such as 92, 108, etc. are observed to be included in the family of problem's optimum configurations.

4.2.1. Matching family of optimum indices to the design point variables

To demonstrate the suitability of the optimum configurations, we select from the joint intersection indices 92 and 107. These configurations will be checked against the randomly selected configurations 33 and 195. The four configuration indices (92, 107, 33 and 195) are matched against the configuration group design spaces in Figure 4, Figure 5 and Figure 6 to derive Table 9. Table 10 is developed by re-arranging Table 9, such that each row represents a unique SLWR configuration. The randomly selected configurations are highlighted in red.

Table 9. Selected configuration design variable table.

Conf. index	Conf. group 1			Conf. group 2			Conf. group 3		
	y_{sag}(m)	AMR	Δh(m)	y_{sag}(m)	AMR	Δh(m)	y_{sag}(m)	AMR	Δh(m)
92	430	-1.5	-	-	-1.5	280	430	-	240
107	490	-1.75	-	-	-1.75	320	490	-	280
33	250	-0.5	-	-	-0.5	160	250	-	80
195	730	-3.25	-	-	-3.25	480	730	-	520

Table 10. Expanded configuration table.

S/N	Conf. ID	Configurations input variables		
		y_{sag}(m)	AMR	Δh(m)
1	92a	430	-1.5	280
2	92b	430	-1.5	240
3	107a	490	-1.75	320
4	107b	490	-1.75	280
5	33a	250	-0.5	160
6	33b	250	-0.5	80
7	195a	730	-3.25	480
8	195b	730	-3.25	520

4.2.2. Output geometric and configuration analysis for the selected optimum configurations

The static configurations of the SLWRs presented in Table 10 are shown in Figure 7. The selected optimum configurations (92a, 92b, 107a, 107b) are observed to cluster around each other. On the other

hand, the profiles of the randomly selected configurations (conf. 33a, conf.33b, conf. 195a, conf. 195b) are found to deviate widely from those of the optimum solution cluster. Bar plot of the geometric output variable (s_b and S_T) of the configurations are presented in Figure 8. The s_b and S_T values of the randomly selected configurations are observed to be higher than those of the optimum configurations, except s_T of conf 33b and s_b of configuration 195a and 195b. Numerical values are presented in Table 11.

One of the cost drivers of the SLWR is the buoyancy material volume of the buoyant section. The smeared volume, vol_b, can be expressed in terms of t_b, s_b, as shown in equation (16). Recall from equation (16) that t_b and s_b are part of the design output variables to be optimised. Hence, optimising t_b and s_b implies optimization of vol_b.

$$vol_b = \pi t_b s_b (OD + t_b) \tag{16}$$

The bar plot of vol_b is presented in Figure 9. While the smeared buoyancy of configuration 195 requires a higher volume to achieve higher wave bend elevation, configuration 33 require lower buoyancy volume because of its lower wave bend elevation, compared with the selected optimum configurations. However, the problem is set to optimise six output variables (not just s_b and S_T), it will therefore be comprehensive to examine the suitability of the selected optimum configurations in terms of all the six variables.

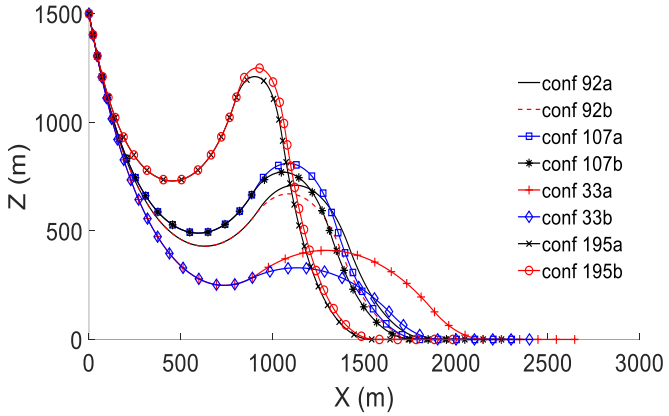

Figure 7. Static configuration of selected SLWRs.

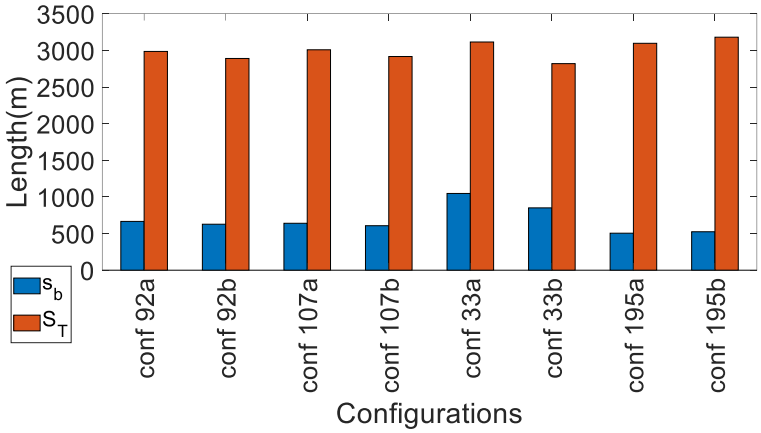

Figure 8. Comparing SLWR hanging length (s_T) and smeared buoyancy section length (s_b).

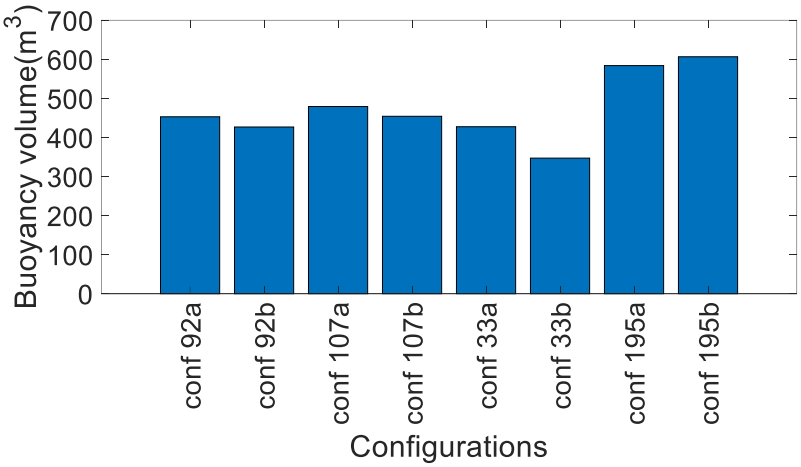

Figure 9. Comparing the volume of SLWRs buoyancy section.

4.2.3. Irregular wave analysis for the selected optimum configuration

The irregular wave loads for combined and fatigue were simulated on the selected SLWR configurations. Figure 10, Figure 11 and Figure 12 respectively present the U_{bend} , the T_{top} and minimum fatigue life of the selected SLWR configurations. Table 11 offers a comparison of maximum values for the design output variables.

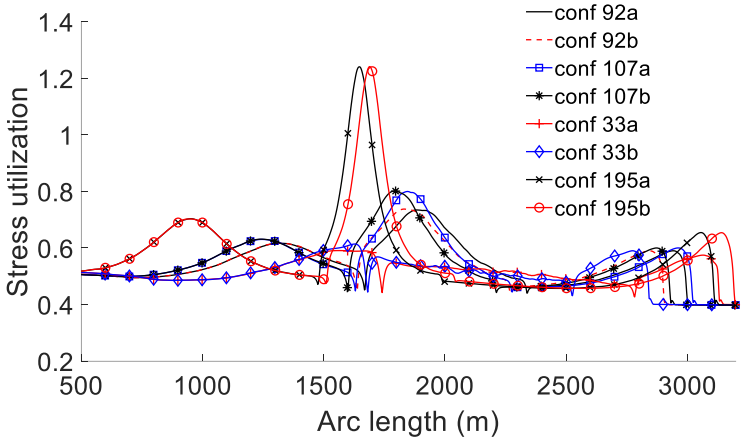

Figure 10. Maximum stress utilization at bends.

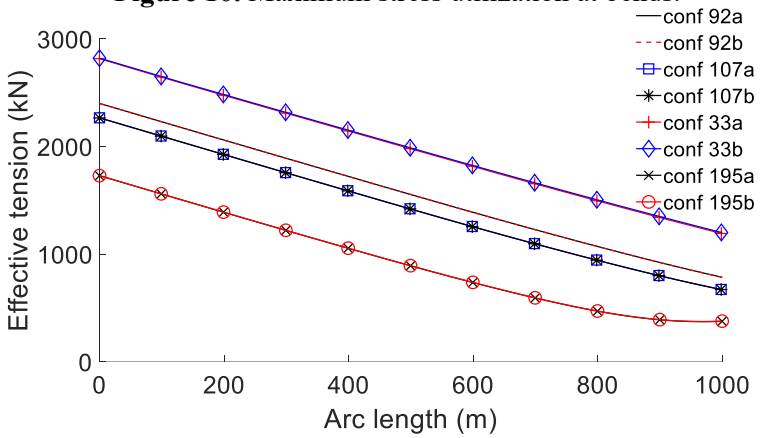

Figure 11. Maximum top tension.

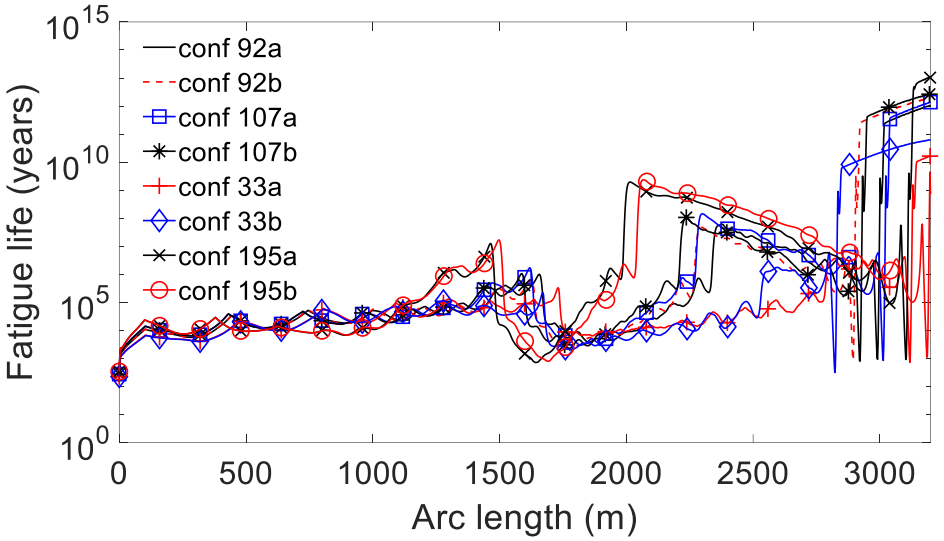

Figure 12. Maximum stress range around SLWR bends.

Table 11. Summary of the configurations output variable.

Conf. ID	Independent Input design variables				Critical values of design output variables					
	y_{sag}(m)	AMR	Δh(m)	U_{bend}	T_{top} (MN)	Min. Life (years)	s_b (m)	S_T (m)	t_b(m)	Vol_b (m^3)
92a	430	-1.5	280	0.75	2400.12	254.68	665.87	2986.01	0.34	452.76
92b	430	-1.5	240	0.75	2399.38	256.31	627.47	2890.03	0.34	426.66
107a	490	-1.75	320	0.80	2266.57	277.88	640.42	3008.41	0.36	479.01
107b	490	-1.75	280	0.80	2265.41	277.87	607.04	2916.61	0.36	454.04
33a	250	-0.5	160	0.77	2815.55	226.24	1047.43	3114.76	0.24	427.32
33b	250	-0.5	80	0.77	2820.92	226.13	850.52	2819.41	0.24	346.99
195a	730	-3.25	480	1.24	1728.75	346.59	504.99	3097.08	0.47	583.74
195b	730	-3.25	520	1.24	1729.24	344.97	524.58	3180.36	0.47	606.38

For easy comparison of the performances of the optimum configurations, the values of the output variable for the randomly selected configurations are compared with the mean values of the optimum configuration. The comparison is expressed in percentages presented in Table 12. Positive percentages mean that the value of the randomly selected configuration output variables is higher than the mean of the values of the optimum configurations. The reverse is the case for negative values. The results show that the 2D optimisation technique balances the interest of all six output variables in the selected optimum configurations. For example, while the mean of the fatigue lives of the optimum configurations is lower than those of the randomly selected configuration 33a and 33b by 15%, the top tension of configuration 33a and 33b are higher by 21%. On the other hand, the randomly selected configuration 195a and 195b have stress utilization higher than the mean stress utilization of the optimum configuration by 60%, but with fatigue life higher by about 30% and a reduction in top tension by about 26%. The results indicate the challenges inherent in solving a multi-objective optimisation problem. A unique decision would be possible for a single-objective optimisation problem. However, for a multi-objective problem, with additional considerations from the designer, a given optimum configuration can be selected from the family of optimum solutions. For example, if the design interest is majorly the cost of the SLWR, the total riser length and volume of buoyancy material will be of interest and configuration 195a and 195b will be seen to be more expensive relative

to the current sets optimum configurations. If the designer's major interest is the top tension capacity of the supporting structure for the riser, then configuration 33a and 33b will be seen to provide higher top tension relative to the current sets of optimum configurations. However, for the above two conditions specified, the 2D tabular technique can be reapplied for the subset of considerations and new sets of optimum configuration can be derived for the problem (see the example presented by equation (12)).

Table 12. Percentage change in critical values of the randomly selected configuration relative to the mean of the optimum configuration.

Conf. ID	Independent Input design variables			% change						
	y_{sag}(m)	AMR	Δh(m)	U_{bend}	T_{top}	Min. Life	s_b	S_T (m)	t_b	Vol_b
33a	250	-0.5	160	-0.6	20.7	-15.2	64.9	5.6	-31.4	-5.7
33b	250	-0.5	80	-0.6	20.9	-15.2	33.9	-4.4	-31.4	-23.4
195a	730	-3.25	480	60.0	-25.9	30.0	-20.5	5.0	34.3	28.8
195b	730	-3.25	520	60.0	-25.9	29.4	-17.4	7.8	34.3	33.8

Note: Positive percentages means that the value of the randomly selected configuration output variables is higher than the mean of the values of the optimum configurations. The reverse is the case for negative values.

5. Conclusion

A 2D tabular optimisation technique is presented in this paper. The technique reduces a higher dimensional design space of a problem to sets of two-dimensional design spaces. It then assigns indices (identifiers) to every design point or configuration in the 2D design spaces. The optimum design points are then tracked through index matching, using techniques such as data sorting and intersection operations.

The technique is demonstrated by its application to solve the SLWR riser optimisation problem. For the SLWR example, there are three independent design input variables: y_{sag}, AMR and Δh. The output variables to be optimised are T_{top}, U_{bend}, s_b, S_T, t_b and $\Delta\sigma$ or fatigue damage. Design points or configurations in the 2D design spaces are simulated with the combined and fatigue wave loads. The design output results are post-processed and organized in a system of result tables or columns, $Y_{p,n}$. A corresponding system of index tables or columns, $I_{p,n}$ is set up, which serve as identifiers for results tables in $Y_{p,n}$. The results columns are sorted in ascending order (for minimisation problem), while the system of index tables is re-arranged accordingly to match the new positions for design points in the sorted result columns. The intersection operation is carried out on the index table system, and the first sets of intersected indices indicate the sets of design points or configuration which optimises the design output variables. A few numbers of selected optimum SLWR configurations, along with some randomly selected configurations, were simulated for 3hrs, using the irregular combined and fatigue wave loads. This is conducted to demonstrate the potential of the technique to capture optimum design configuration for the problem. The results showed that the 2D tabular technique could take into consideration a balance of the interest of all output variables, by reporting indices for configurations, which equally optimises the design output. The 2D tabular method is also able to report new sets of configuration candidates if the search criteria or the set of design output variables to be optimised is changed. The tabular approach has robust potentials to cut down computation resources required for a higher dimensional problem. It can also accommodate additional load scenarios and other external design constraints that may be imposed on the optimization process.

6. Recommendation

In the SLWR optimisation example demonstrated in this paper, the tabular optimisation technique reduces the three-dimensional problem to two dimensions. A potential limitation with the technique is with the reduction of higher dimensional space to that of two dimensions, a transformation which needs further investigation. Future work will be to extend this technique to higher dimensional riser optimisation problems. This could significantly improve the efficiency in the riser optimisation computation.

7. Acknowledgement

The authors acknowledge the support of the University of Strathclyde and McDermott International for their support. Results in this work were obtained using the ARCHIE-WeST High-Performance Computer (www.archie-west.ac.uk) based at the University of Strathclyde.

References

[1] Clukey E, Ghosh R, Mokarala P and Dixon M Steel catenary riser (SCR) design issues at touch down area. Int. Society of Offshore and Polar Engineers)
[2] Song R and Stanton P Advances in Deepwater Steel Catenary Riser Technology State-of-the-Art: Part I—Design. American Society of Mechanical Engineers)
[3] Quintin H, Legras J-L, Huang K and Wu M 2007 Steel catenary riser challenges and solutions for deepwater applications. In: *Offshore Tech. Conf.*: (Houston, Texas: Offshore Tech. Conf.)
[4] Quéau L M, Kimiaei M and Randolph M F 2015 Sensitivity studies of SCR fatigue damage in the touchdown zone using an efficient, simplified framework for stress range evaluation *Ocean Engineering* 96 295-311
[5] Gore C T and Mekha B B 2002 Common Sense Requirements (CSRs) for Steel Catenary Risers (SCRs). In: *Offshore Tech. Conf.,* (Houston, Texas: Offshore Tech. Conf.)
[6] Ogbeifun A M, Oterkus S, Race J, Naik H, Decnop E and Dakshina M The Branched Riser Systems: Concept Development. In: *ASME 2019 38th Int.Conf. on Ocean, Offshore and Arctic Engineering*: (American Society of Mechanical Engineers Digital Collection)
[7] Li S and Nguyen C 2010 Dynamic response of deepwater lazy-wave catenary riser *Deep Offshore Tech. Int., Amsterdam, The Netherlands*
[8] Standard D-O F201, 2010 *Dynamic Risers. DNV: Norway*
[9] Veritas D N 2011 Modelling and analysis of marine operations *Offshore Standard*
[10] Randolph M and Quiggin P 2009 Non-linear hysteretic seabed model for catenary pipeline contact. In: *ASME 2009 28th Int. Conf. on Ocean, Offshore and Arctic Eng.*: (American Society of Mechanical Engineers)
[11] Manual O 2012 Online at http://www. orcina. com/SoftwareProducts/OrcaFlex/Documentation *OrcaFlex. pdf*
[12] Heffernan D 2016 An introduction to the Python interface to OrcaFlex. Orcina, Tech. Rep